Positron scattering and annihilation from hydrogenlike ions

S. A. Novikov, M. W. J. Bromley,[*] and J. Mitroy[†]

Faculty of TIE, Charles Darwin University, Darwin NT 0909, Australia

(Received 10 December 2003; published 4 May 2004)

The Kohn variational method is used with a configuration-interaction-type wave function to determine the $J=0$ and $J=1$ phase shifts and annihilation parameter Z_{eff} for positron-hydrogenic ion scattering. The phase shifts are within $1-2\%$ of the best previous calculations. The values of Z_{eff} are small and do not exceed unity for any of the momenta considered. At thermal energies Z_{eff} is minute with a value of order 10^{-50} occurring for He$^+$ at $k=0.05a_0^{-1}$. In addition to the variational calculations, analytic expressions for the phase shift and annihilation parameters within the Coulomb wave Born approximation are derived and used to help elucidate the dynamics of positron collisions with positive ions.

I. INTRODUCTION

The scattering of positrons from atomic ions is not a problem that has received much attention. There are a variety of reasons for this. On the experimental side, the difficulties in working with positron beams are well known and there has never been an experiment upon such a system. From the theoretical side, the asymptotic form of the wave function involves Coulomb waves which have more complicated analytic forms than plane waves. For example, some methods used in the momentum space solutions of the Lippmann-Schwinger equation for positron-hydrogen scattering [1,2] are not easily adapted to the positron-He$^+$ system.

When it comes to calculations of the positron-He$^+$ system, one can literally count the different calculations on one hand. The first published calculations treated electron-positron correlations realistically, but were not large enough to achieve convergence [3]. More recently, Bransden *et al.* [4] solved the Lippmann-Schwinger equation in a mixed basis of e^+-He$^+$ and Ps-He^{2+} channels to obtain relatively accurate phase shifts for the positron-He$^+$ system. Most recently, the Harris-Nesbet variational method has been applied by Gien to give phase shifts for positron scattering for the various ions (He$^+$, Li^{2+}, Be^{3+}, and B^{4+}) in the elastic-scattering region [5,6].

In the present paper, the Kohn variational method is applied to the problem of positron scattering from hydrogenic ions. Unlike some other applications of the Kohn method to simple systems [5,7,8], the present approach does not include basis functions with interelectronic coordinates and instead uses a basis of functions all centered on the nucleus. The use of such a configuration-interaction (CI) -type basis does entail some large-scale calculations, but the issues involved in doing these calculations at low energies have been effectively solved [9]. The only changes that had to be made to the program used for the positron-hydrogen system were the replacement of the long-range spherical Bessel function type

basis functions with Coulomb functions. Besides presenting *s*- and *p*-wave phase shifts, an analysis of positron annihilation during the collision is also presented. Initially, the Coulomb wave Born approximation (CWBA) is used to show that the positron annihilation rate is largely dominated by the ability of the positron to tunnel through the repulsive Coulomb interaction. The annihilation parameter Z_{eff} is then computed using the wave functions obtained from the variational calculation.

II. DETAILS OF THE CALCULATION

A. The scattering Hamiltonian

The interaction Hamiltonian for positron-hydrogen-like ions is written as

$$H = -\frac{1}{2}\nabla_0^2 + \frac{Z}{r_0} - \frac{1}{2}\nabla_1^2 - \frac{Z}{r_1} - \frac{1}{r_{01}}. \quad (1)$$

Since the target system only contains one electron, the asymptotic potential exerted on the positron at long distances from the nucleus is $(Z-1)/r_0$.

B. The Kohn variational method and trial wave function

The Kohn variational method [10–12] is a commonly used method to solve the Schrödinger equation for low-energy-scattering problems. The CI-Kohn formalism presented here closely follows that outlined in Ref. [9], which was based on the exposition in the monograph of Burke and Joachain [13].

The CI-type trial wave function adopted for the present Kohn variational calculations has the form

$$|\Psi;JM_J\rangle = \alpha_0|\Phi_s;JM_J\rangle + \alpha_1|\Phi_c;JM_J\rangle + \sum_{i,j} c_{ij}|\Phi_{ij};JM_J\rangle,$$

$$(2)$$

where the first two terms involve continuum functions that are equal to the regular and irregular Coulomb functions, at large distances from the origin. The three types of functions are written as

---

[*]Present address: Department of Physics, Kansas State University, Manhattan, KS 66506, USA.

[†]Electronic address: jxm107@rsphysse.anu.edu.au

$$|\Phi_{ij};JM_J\rangle = \sum_{m_i,m_j} \langle \ell_i m_i \ell_j m_j | JM_J \rangle \phi_i(\mathbf{r}_1)\phi_j(\mathbf{r}_0), \quad (3)$$

$$|\Phi_s;JM_J\rangle = \sum_{m_{g.s.},m} \langle \ell_{g.s.} m_{g.s.} \ell m | JM_J \rangle \phi_{g.s.}(\mathbf{r}_1)\theta_s(\mathbf{r}_0), \quad (4)$$

$$|\Phi_c;JM_J\rangle = \sum_{m_{g.s.},m} \langle \ell_{g.s.} m_{g.s.} \ell m | JM_J \rangle \phi_{g.s.}(\mathbf{r}_1)\theta_c(\mathbf{r}_0). \quad (5)$$

In these expressions, $\phi_i(\mathbf{r}_1)$ and $\phi_j(\mathbf{r}_0)$ are short-range square integrable functions with orbital angular momenta ℓ_i and ℓ_j. The function, $\phi_{g.s.}(\mathbf{r}_1)$ is the ground-state (g.s.) wave function of the target ion, while $\theta_s(\mathbf{r}_0)$ and $\theta_c(\mathbf{r}_0)$ are the continuum functions. Considerations of spin have been omitted from the wave function since they exert no impact upon the scattering wave function. Since the target ion ground state has $\ell_{g.s.}=0$, considerations of angular-momentum conservation require that $\ell=J$. The radial parts of the positron continuum functions have the form

$$\theta_s(r_0) = F_J(\eta, kr_0), \quad (6)$$

$$\theta_c(r_0) = [1 - \exp(-\beta r_0)]^{2J+1} G_J(\eta, kr_0). \quad (7)$$

For hydrogenlike ions $\eta=(Z-1)/k$. For neutral atoms $\eta=0$, and the Coulomb functions are reduced to spherical Bessel functions: $F_J(0,kr)=krj_J(kr)$ and $G_J(0,kr)=-krn_J(kr)$. The $[1-\exp(-\beta r_0)]^{2J+1}$ factor is used to make the irregular solution $\theta_c(r_0)$ go to zero as $r_0 \to 0$. The factor β was generally set to 2.0 for the present calculations. The scattering lengths and annihilation parameter Z_{eff} were insensitive to the precise value chosen for β. The short-range functions $\phi_i(\mathbf{r}_1)$ and $\phi_j(\mathbf{r}_0)$ are written as a linear combination of Laguerre-type orbitals (LTOs). All the basis functions so far, except $|\Phi_s;JM_J\rangle$ and $|\Phi_c;JM_J\rangle$, are identical in functional form to the basis functions used in earlier CI-Kohn calculations of positron-hydrogen and positron-copper scattering [9].

The asymptotic form of the scattering wave functions can be written with a number of different normalizations [14] depending on the form adopted for α_0 and α_1. These conditions are

$$\alpha_0 = \cos \tau - \alpha_t \sin \tau, \quad (8)$$

$$\alpha_1 = \sin \tau + \alpha_t \cos \tau, \quad (9)$$

$$\alpha_t = \tan(\delta_t - \tau), \quad (10)$$

where δ_t is the phase shift of the trial wave function and $\tau \in [0, \pi/2]$. When $\tau=0$, α_t reduces to $\tan(\delta_t)$, which is just the K-matrix element. The choice $\tau=\pi/2$ gives $\alpha_t =\cot(\delta_t)$, which is just the reciprocal of K-matrix element. (The choice $\tau=\pi/2$ is sometimes called the inverse Kohn method [15].)

Besides the normalizing condition, there is one other area where there is flexibility in the choice of the continuum functions. This concerns whether the functions θ_s and θ_c are orthogonalized to the short-range L^2 radial basis functions. Ei-

ther choice is permissible, but we chose to orthogonalize since this simplified the evaluation of the matrix elements.

The generalized Kohn functional $\alpha_v=\tan(\delta_v-\tau)$ is given by

$$\alpha_v = \alpha_t - 2\langle \Psi_t | H - E | \Psi_t \rangle. \quad (11)$$

Applying the Kohn condition that the Kohn functional is stationary with respect to the linear variational parameters in the trial wave function leads to the linear equations

$$\frac{\partial \alpha_v}{\partial \alpha_t} = 0, \quad (12)$$

$$\frac{\partial \alpha_v}{\partial c_i} = 0, \quad i = 1, 2, \ldots, N_{SR}, \quad (13)$$

where N_{SR} is the total number of short-range basis functions. These equations are solved to determine α_t and c_i. The error in α_v upon solving the set of $(N_{SR}+1)$ linear equations is of second order with respect to variations in the trial wave function.

Besides the phase shift, the annihilation parameter Z_{eff} is also calculated. The spin-averaged annihilation parameter can be written as [16–18]

$$Z_{eff} = N \int d^3 r_0 d^3 r_1 |\Psi(\mathbf{r}_0,\mathbf{r}_1)|^2 \delta(\mathbf{r}_0 - \mathbf{r}_1), \quad (14)$$

where $\Psi(\mathbf{r}_0,\mathbf{r}_1)$ is the total wave function of the system. In the plane-wave Born approximation, the positron wave function is written as a plane wave and the annihilation parameter is equal to the number of atomic electrons, i.e., $Z_{eff}=N_e$.

The partial-wave contributions to Eq. (14),

$$Z_{eff} = \sum_{J=0}^{\infty} Z_{eff}^{(J)}, \quad (15)$$

can be written as

$$Z_{eff}^{(J)} = N_k \sum_{i,j=1}^{N_{CI}} c_i c_j \int r\phi_{a_i}(r) r\phi_{a_j}(r) \phi_{p_i}(r) \phi_{p_j}(r)dr$$
$$\times \sum_{k=k_{min}}^{k_{max}} (2k+1)\langle \phi_{a_i}\phi_{p_i};J\|\mathbf{C}^k(\hat{\mathbf{r}}_1) \cdot \mathbf{C}^k(\hat{\mathbf{r}}_0)\|\phi_{a_j}\phi_{p_j};J\rangle, \quad (16)$$

where $N_{CI}=(N_{SR}+2)$ is total number of basis functions. The functions $\phi_{a_i}(r)$, $\phi_{p_i}(r)$, etc., are the radial parts of the single electron and positron orbitals. The coefficients α_0 and α_1 of the two continuum basis functions are evaluated from α_t [using Eq. (10)] for a specific value of τ. The factor N_k is defined as

$$N_k = \frac{1}{k(\alpha_0^2 + \alpha_1^2)}. \quad (17)$$

The L^2 basis was constructed by populating all the possible configurations that could be formed by letting the electron and positron populate all the orbitals subject to the selection rules,

$$\max (\ell_i, \ell_j) \leq L_{max}, \qquad (18)$$

$$|\ell_i - \ell_j| \leq J, \qquad (19)$$

$$(-1)^{\ell_i + \ell_j} = (-1)^J. \qquad (20)$$

In these expressions ℓ_j is the positron angular momentum and ℓ_i is the electron angular momentum. It is necessary to choose a basis with a large value of L_{max} in order to obtain results close to convergence. It is known that the attractive interaction between the electron and positron leads to localization of the atomic electrons in the vicinity of the positron [19,20]. The formation of something akin to a virtual Ps cluster leads to very slow convergence with ℓ. The convergence of Z_{eff} with respect to L_{max} is typically much slower than the phase shift.

The slow convergence of the phase shift and annihilation rate with increasing L_{max} means an extrapolation technique must be used to estimate the $L_{max} \to \infty$ limit. Making the assumption that the successive increments to an physical observable X_L scale as $1/L^p$ for sufficiently large L, one can write

$$X_\infty = \lim_{L_{max} \to \infty} \left(X_{L_{max}} + \Delta \sum_{L=L_{max}+1}^{\infty} \frac{1}{L^p} \right). \qquad (21)$$

The power series is easy to evaluate, the coefficient Δ is defined as

$$\Delta = (X_{L_{max}} - X_{L_{max}-1})(L_{max})^p, \qquad (22)$$

and the exponent p can be derived from

$$\left(\frac{L_{max}}{L_{max}-1} \right)^p = \frac{X_{L_{max}-1} - X_{L_{max}-2}}{X_{L_{max}} - X_{L_{max}-1}}. \qquad (23)$$

Recently Gribakin and Ludlow [21] using second-order perturbation theory to study bound positron-atom complexes showed that the energy exponent p_E was 4, while the exponent for the annihilation rate, p_Γ, was 2. Translating these results to the scattering region suggests that p_δ should be 4 while p_Z should be 2. In practice, the exponents obtained in large-scale calculations are usually slightly smaller than the expected values [9,22,23].

One criticism of the present ansatz is that the single-center trial wave function does not explicitly include the electron-positron coordinate. However, this deficiency is rectified by the use of high ℓ components in the wave function. For example, positron-hydrogen phase shifts computed with the CI-Kohn formalism agree with the best variational phase shifts to an accuracy of 10^{-3} rad [9]. The accuracy achieved for Z_{eff} is not quite as good, but even here agreement at the 5% level was achieved [9].

III. THE COULOMB WAVE BORN APPROXIMATION

The CWBA is the simplest of all approximations used in the paper. The expression for the phase shift δ_J is

$$\tan \delta_J = -\frac{2}{k} \int_0^\infty F_J^2(\eta, kr_0) e^{-2Zr_0} \left(\frac{1}{r_0} + Z \right) dr_0, \qquad (24)$$

where the regular Coulomb function is defined as usual in terms of the confluent hypergeometric function [24]

$$F_J(\eta, kr_0) = \frac{2^J e^{-(1/2)\pi\eta}}{(2J+1)!} |\Gamma(J+1+i\eta)| e^{-ikr_0}(kr_0)^{J+1}$$

$$\times M(J+1-i\eta, 2J+2, 2ikr_0). \qquad (25)$$

In order to evaluate the integrals we use the identity [25]

$$V = \int_0^\infty e^{-\lambda x} x^{\gamma-1} M(\alpha, \gamma, kx) M(\alpha', \gamma, k'x) dx$$

$$= \Gamma(\gamma) \lambda^{\alpha+\alpha'-\gamma} (\lambda - k)^{-\alpha} (\lambda - k')^{-\alpha'}$$

$$\times {}_2F_1 \left(\alpha, \alpha'; \gamma; \frac{kk'}{(\lambda-k)(\lambda-k')} \right), \qquad (26)$$

and make use of parametric differentiation to develop

$$\int_0^\infty e^{-\lambda x} x^\gamma M(\alpha, \gamma, kx) M(\alpha', \gamma, k'x) dx = -\frac{dV}{d\lambda}. \qquad (27)$$

Finally, making use of

$$\left(\frac{\mu+i}{\mu-i} \right)^{i\mu} = e^{-2\mu \arctan(1/\mu)}, \qquad (28)$$

where $\mu = Z/k$ leads to

$$\tan \delta_J = -\frac{1}{2k} W(\eta) \frac{e^{2\eta \arctan(1/\mu)}}{(1+\mu^2)^{J+2}} \sum_{n=0}^{\infty}$$

$$\times \frac{1+\mu^2(n+J+2+\eta/\mu)}{n!(n+2J+1)!(1+\mu^2)^n} \frac{1}{\eta^2} \prod_{s=0}^{n+J} (s^2 + \eta^2), \qquad (29)$$

with $W(\eta) = 2\pi\eta/(e^{2\pi\eta}-1)$.

For the CWBA, Eq. (14) collapses to

$$Z_{eff} = \int d^3r_0 d^3r_1 |\psi_{\mathbf{k}}(\mathbf{r}_0) \phi_{1s}(\mathbf{r}_1)|^2 \delta(\mathbf{r}_0 - \mathbf{r}_1). \qquad (30)$$

Using the partial-wave decomposition for the three-dimensional Coulomb scattering function (with σ_l set to the Coulomb phase shift)

$$\psi_{\mathbf{k}}(\mathbf{r}_0) = \frac{1}{kr_0} \sum_{l=0}^{\infty} (2l+1) i^l e^{i\sigma_l} F_l(\eta, kr_0) P_l(\hat{\mathbf{k}} \cdot \hat{\mathbf{r}}_0) \qquad (31)$$

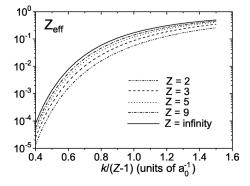and the standard expansion for the delta function

FIG. 1. The CWBA annihilation parameter Z_{eff} vs the scaled momentum $k/(Z-1)$ (in units of a_0^{-1}) for $Z=2,3,5,9$, and ∞. The size of Z_{eff} increases monotonically with Z for the range of momentum considered.

$$\delta(\mathbf{r}_0 - \mathbf{r}_1) = \frac{1}{4\pi r_1^2}\delta(r_0 - r_1)\sum_{k=0}^{\infty}(2k+1)\mathbf{C}^k(\hat{\mathbf{r}}_1)\cdot\mathbf{C}^k(\hat{\mathbf{r}}_0),$$

(32)

one obtains

$$Z_{eff}^{(J)} = \frac{4Z^3}{k^2}(2J+1)\int_0^{\infty}F_J^2(\eta,kr_0)e^{-2Zr_0}dr_0.$$

(33)

Using the reduced variable $x=kr_0$, this simplifies to

$$Z_{eff}^{(J)} = 4\mu^3(2J+1)\int_0^{\infty}F_J^2(\eta,x)e^{-\mu x}dx.$$

(34)

Once Eq. (25) is inserted into Eq. (34) and use is made of Eqs. (27) and (28) one gets

$$Z_{eff}^{(J)} = (2J+1)W(\eta)\frac{e^{2\eta\,\arctan(1/\mu)}}{(1+\mu^2)^{J+2}}\mu^4$$
$$\times\sum_{n=0}^{\infty}\frac{n+J+1+\eta/\mu}{n!\,(n+2J+1)!\,(1+\mu^2)^n}\frac{1}{\eta^2}\prod_{s=0}^{n+J}(s^2+\eta^2).$$

(35)

The CWBA estimates of the phase shift and Z_{eff} are given in Tables III–X for selected values of k. The values of k have been chosen so that entries of different Z are often given at the same values of η. These estimates of the δ_J and $Z_{eff}^{(J)}$ were computed independently with two different methods. First of all, Eqs. (29) and (35) were evaluated by summing the power series. In addition, Eqs. (24) and (33) were integrated using Gaussian quadratures. The two methods gave numerical results in agreement to better than ten significant digits.

Figure 1 plots the CWBA estimate of the total Z_{eff} versus the scaled momentum $1/\eta=k/(Z-1)$ for $Z=2,3,5,9$, and ∞. For no species does Z_{eff} exceed 1.0 at any momentum considered. The increase in Z_{eff} with k reflects the fact that a positron is better able to tunnel through the repulsive Coulomb field at higher energies. Figure 1 does not show values of Z_{eff} below $1/\eta=0.4a_0^{-1}$ since Z_{eff} becomes minute at smaller k values and therefore it would be difficult to sepa-
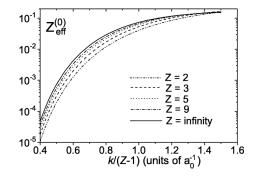

FIG. 2. The CWBA annihilation parameter $Z_{eff}^{(0)}$ vs the scaled momentum $k/(Z-1)$ (in units of a_0^{-1}) for $Z=2,3,5,9$, and ∞.

rate the curves for different Z on the plot. To put the minute size for He$^+$ into perspective, $Z_{eff}^{(0)}=1.66\times10^{-52}$ and $Z_{eff}^{(1)}=3.10\times10^{-53}$ at $k=0.05a_0^{-1}$. The vanishingly small size of $Z_{eff}^{(J)}$ is easily explained in terms of physical considerations. The classical turning radius for a $J=0$ positron incident upon He$^+$ at $k=0.05a_0^{-1}$ is $(Z-1)/k^2=400a_0$. For the positron to annihilate with the electron it has to tunnel almost $400a_0$ through a Coulomb barrier that gets increasingly more repulsive as it approaches the nucleus. The rapid variation of Z_{eff} at small values of $1/\eta$ seen in Fig. 1 reflects the change in the size of classical forbidden region, and therefore a change in the tunneling distance, as the energy changes. The steadily decreasing amplitude of the positron wave function close to the origin due to tunneling is reflected mathematically by the $W(\eta)$ factor in Eq. (35).

It is also noted that the size of Z_{eff} at constant $1/\eta$ increases monotonically with Z for the range of momentum considered. This is discussed in more detail later.

Figure 2 plots the s-wave annihilation parameter $Z_{eff}^{(0)}$ versus $1/\eta$ for $Z=2,3,5,9$, and ∞. When $1/\eta$ is fixed, there is a tendency for $Z_{eff}^{(0)}$ to increase monotonically with Z. However, the curves tend to intersect at $1/\eta\approx1.5$ and for $1/\eta>2$ (not depicted on the graph) $Z_{eff}^{(0)}$ decreases monotonically with Z.

A. Analytic expressions for Z_{eff} when $\eta=0$

The expressions for $Z_{eff}^{(J)}$ reduce to much simpler forms for positron-hydrogen scattering. In this case $\eta=0$, Eq. (35) for s-wave scattering becomes

$$Z_{eff}^{(0)} = \frac{\mu^2}{1+\mu^2}.$$

(36)

For p-wave scattering, analytic evaluation is still possible but the answer is somewhat more complicated:

$$Z_{eff}^{(1)} = \frac{3\mu^2}{(1+\mu^2)^2} + 6\mu^4\left[\ln\left(\frac{\mu^2}{1+\mu^2}\right)+\frac{1}{1+\mu^2}+\frac{1}{2(1+\mu^2)^2}\right].$$

(37)

These expressions are only presented for completeness since no calculations are presented for hydrogen.

TABLE I. The coefficients of the power-series expansion in $k^2/(Z-1)^2$, Eq. (38) of $Z_{\text{eff}}^{(J)}$.

Z	ν	a_0	a_1	a_2	b_0	b_1	b_2
2	0.500	4.9778	0.9262	0.02613	−2.0254	0.4641	0.1147
3	0.66$\dot{6}$	8.8109	2.6115	0.1257	−7.2369	0.08679	0.4830
5	0.800	14.0408	5.4829	0.3670	−18.2063	−2.6695	1.1924
9	0.88$\dot{8}$	19.2296	8.7363	0.7046	−32.5939	−7.9946	1.9504
∞	1.00	28.5973	15.2720	1.5112	−65.6166	−23.6940	3.1152

B. The $k \to 0$ limit for $Z_{\text{eff}}^{(J)}$

The behavior of $Z_{\text{eff}}^{(J)}$ for positive ions at low values of k can be written as

$$Z_{\text{eff}}^{(J)} \simeq W(\eta)\left[a_J(\nu) + b_J(\nu)\frac{k^2}{(Z-1)^2} + O(k^4)\right], \quad (38)$$

where $\nu=(Z-1)/Z$ and

$$a_J(\nu) = (2J+1)e^{2\nu}\nu^{2J}\sum_{n=0}^{\infty}\frac{n+J+1+\nu}{n!\,(n+2J+1)!}\nu^{2n}, \quad (39)$$

$$b_J(\nu) = (2J+1)e^{2\nu}\nu^{2J}\sum_{n=0}^{\infty}\frac{n+J+1+\nu}{n!\,(n+2J+1)!}\nu^{2n}$$
$$\times\left[\frac{(n+J)(n+J+1)(2n+2J+1)}{6}\right.$$
$$\left. -(n+J+2)\nu^2 - \frac{2}{3}\nu^3\right]. \quad (40)$$

Some typical values of a_J and b_J are listed in Table I. The interesting feature of this analysis is that the s, p, and d waves have terms in the power-series expansion of $Z_{\text{eff}}^{(J)}$ in the same order of k^2. However, the s-wave coefficient $a_0(\nu)$ is larger than the p-wave coefficient $a_1(\nu)$, which is in turn larger than the d-wave coefficient $a_2(\nu)$. Although values have not been tabulated, the higher partial waves also have terms of the same order in the power-series expansion.

The energy dependence of $Z_{\text{eff}}^{(J)}(k)$ is to a very large extent determined by the reciprocal of the scaled momentum $\eta = (Z-1)/k$ through the $W(\eta)$ factor.

C. The $Z \to \infty$ limit for $Z_{\text{eff}}^{(J)}$

The limit for $Z_{\text{eff}}^{(J)}$ as $Z \to \infty$ is well defined, provided the limit is taken under the constraint that $\eta=(Z-1)/k$ remains constant. It is possible to show that

$$Z_{\text{eff}}^{(J)}(\eta) \simeq \Lambda_0(J,\eta) + \frac{\Lambda_1(J,\eta)}{Z-1} + O((Z-1)^{-2}). \quad (41)$$

The coefficient $\Lambda_0(J,\eta)$ only depends on η as $\mu \to \eta$ and $Z \to \infty$:

$$\Lambda_0(J,\eta) = (2J+1)W(\eta)\frac{e^{2\eta\,\arctan(1/\eta)}}{(1+\eta^2)^{J+2}}\,\eta^2$$
$$\times\sum_{n=0}^{\infty}\frac{n+J+2}{n!\,(n+2J+1)!}\frac{1}{(1+\eta^2)^n}$$
$$\times\prod_{s=0}^{n+J}(s^2+\eta^2). \quad (42)$$

The leading correction $\Lambda_1(J,\eta)$ is

$$\Lambda_1(J,\eta) = 4(2J+1)W(\eta)\frac{e^{2\eta\,\arctan(1/\eta)}}{(1+\eta^2)^{J+2}}\,\eta^2\sum_{n=0}^{\infty}\left[n+J+7/4\right.$$
$$\left. -\frac{\eta^2}{1+\eta^2}\frac{(n+J+2)(n+J+3)}{2}\right]$$
$$\times\frac{1}{n!\,(n+2J+1)!}\frac{1}{(1+\eta^2)^n}\prod_{s=0}^{n+J}(s^2+\eta^2). \quad (43)$$

It is also possible to write $\Lambda_0(J,\eta)$ and $\Lambda_1(J,\eta)$ in terms of the integrals derived from Eq. (34) $(\mu \to \eta)$ as

$$\Lambda_0(J,\eta) = 4\eta^3(2J+1)\int_0^{\infty}F_J^2(\eta,x)e^{-2\eta x}dx \quad (44)$$

and

$$\Lambda_1(J,\eta) = 3\Lambda_0(J,\eta) - 8\eta^4(2J+1)\int_0^{\infty}xF_J^2(\eta,x)e^{-2\eta x}dx. \quad (45)$$

The coefficients $\Lambda_0(J,\eta)$ and $\Lambda_1(J,\eta)$ are tabulated in Table II for a series of η values for $J=0,1$, and 2. It is noticeable that the relative size of the $\Lambda_1(J,\eta)/\Lambda_0(J,\eta)$ ratio decreases as $k/(Z-1)$ increases. The series in Eq. (41) is more quickly convergent at larger values of k.

D. Computation of the Coulomb functions

The asymptotic scattering functions are regular and irregular Coulomb functions. Since all integrations are done numerically this meant that computer programs to calculate Coulomb functions were needed, and the more accurate the functions the better. The necessary values of the Coulomb function were computed with two complementary approaches [26,27].

TABLE II. The coefficients of the power-series expansion in $1/(Z-1)$, Eq. (41) of $Z_{\text{eff}}^{(J)}$. The numbers in square brackets denote powers of 10, therefore a[b] means $a \times 10^b$.

$1/\eta$	$J=0$		$J=1$		$J=2$	
	Λ_0	Λ_1	Λ_0	Λ_1	Λ_0	Λ_1
0.25	0.7610[−8]	−0.2466[−7]	0.4250[−8]	−0.1937[−7]	0.5133[−9]	−0.3200[−8]
0.50	0.7566[−3]	−0.1819[−2]	0.4750[−3]	−0.1742[−2]	0.8588[−4]	−0.4501[−3]
0.75	0.2039[−1]	−0.2981[−1]	0.1493[−1]	−0.3952[−1]	0.3973[−2]	−0.1623[−1]
1.00	0.7371[−1]	−0.4740[−1]	0.6328[−1]	−0.1102	0.2300[−1]	−0.6985[−1]
1.25	0.1255	−0.9403[−3]	0.1250	−0.1272	0.5788[−1]	−0.1261
1.50	0.1528	0.7098[−1]	0.1736	−0.7995[−1]	0.9702[−1]	−0.1457

The program of Seaton [26] evaluates the Coulomb functions by direct evaluation of the power series. As can be expected, such an approach is accurate close to the origin where relatively few terms are required in the power series. At larger values of kr, round-off and series truncation errors in the oscillating terms of the power series become more important and start to limit the accuracy.

The program of Barnett uses an approach based on continued fractions [27]. This continued fraction algorithm is known to be accurate at distances larger than the classical turning point,

$$r_c^J = \frac{Z - 1 + \sqrt{(Z-1)^2 + J(J+1)k^2}}{k^2}. \tag{46}$$

Inside the classical turning point round-off errors have a negative impact upon the reliability of the continued fraction calculation.

There is one aspect about the Seaton program that warrants specific mention. Although this program is stated to be a double precision (i.e., 15 digits) program, the program as published cannot be guaranteed to be this accurate over a variety of architectures. In our initial calculations upon a 32-bit INTEL based Linux workstation it was noticed that the Coulomb functions were only accurate to seven significant digits. The Seaton code did not pay enough attention to the explicit definition of data types to ensure they would be double precision under different architectures (note that the
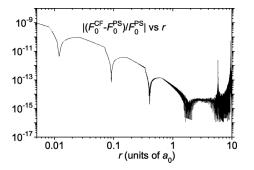
Seaton program was initially developed on the 64-bit ALPHA architecture). Accordingly, various sundry program modifications entailing less than 60 min of editing time had to be made before the program performed to its expected accuracy.

Figures 3 and 4 show a comparison between the continued fraction (CF) and power-series (PS) evaluations of the Coulomb functions. Denoting F_J^{CF}, G_J^{CF} and F_J^{PS}, G_J^{PS} as the two different computational implementations of the regular and irregular Coulomb functions, the quantities plotted are $|F_0^{CF} - F_0^{PS}|/|F_0^{PS}|$ and $|G_0^{CF} - G_0^{PS}|/|G_0^{PS}|$. A plot of the relative differences $|F_1^{CF} - F_1^{PS}|/|F_1^{PS}|$ and $|G_1^{CF} - G_1^{PS}|/|G_1^{PS}|$ for the $J=1$ Coulomb function were not shown since they were almost identical to that for $J=0$.

The increasing degree of inaccuracy in F_J^{CF} and G_J^{CF} at the smallest values of r is readily apparent. There is a complete failure in F_J^{CF} at the smallest values of r, but this is not shown in the figures. There is an extended region of r between $1a_0$ and $5a_0$ where both algorithms are working with close to machine precision. This region straddles the classical turning radius which for the kinematic conditions shown in the figures is $2.0a_0$ for s-wave scattering. Larger fluctuations between F_J^{CF} and F_J^{PS} occur for $r > 5a_0$ when round-off errors in F_J^{PS} become more important.

For the calculations reported in this paper, the PS method was used for $r \leqslant r_c^J/2$ while the CF fraction method was used for $r > r_c^J/2$. A correct choice of the appropriate algorithm was important for small k and high Z. Some calculations

FIG. 3. The relative difference $|F_0^{CF} - F_0^{PS}|/|F_0^{PS}|$ between the Coulomb functions calculated by the continued fraction and power-series algorithms as a function of r. The present curves were plotted for $(Z-1)=1$ and $k=1.0a_0^{-1}$.
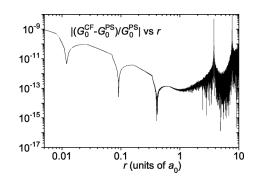

FIG. 4. The relative difference $|G_0^{CF} - G_0^{PS}|/|G_0^{PS}|$ between the irregular Coulomb functions calculated by the continued fraction and power-series algorithms as a function of r. The present curves were plotted using $(Z-1)=1$ and $k=1.0a_0^{-1}$.

TABLE III. The phase shifts δ_J (in radians) for positron scattering from He$^+$. The column k reports momentum in a_0^{-1}. The numbers in square brackets denote powers of 10.

k	CWBA	CC(1)	CC(3)	CC($\bar{3}$)	CIKOHN$_8$[a]	CIKOHN$_\infty$	BNW	Gien (E6PS)	Model
				$J=0$					
0.25	−0.753[−10]	−0.704[−10]	0.1221[−4]	0.1852[−4]	0.1852[−4]	0.1852[−4]			0.1862[−5]
0.50	−0.2032[−4]	−0.1876[−4]	0.4405[−3]	0.6864[−3]	0.7160[−3]	0.7163[−3]			0.7244[−3]
0.75	−0.1219[−2]	−0.1112[−2]	0.1909[−2]	0.3826[−2]	0.4793[−2]	0.4810[−2]	0.473[−2]	0.478[−2]	0.4880[−2]
1.00	−0.8791[−2]	−0.7869[−2]	−0.4418[−3]	0.5430[−2]	0.1023[−1]	0.1031[−1]	0.105[−1]	0.103[−1]	0.1030[−1]
1.25	−0.2703[−1]	−0.2371[−1]	−0.1277[−1]	−0.2343[−2]	0.8374[−2]	0.8554[−2]	0.725[−2]	0.846[−2]	0.7585[−2]
1.50	−0.5429[−1]	−0.4691[−1]	−0.3439[−1]	−0.2070[−1]	−0.4375[−2]	−0.4133[−2]	−0.661[−2]	−0.426[−2]	−0.7747[−2]
				$J=1$					
0.25	−0.424[−11]	−0.361[−11]	0.1112[−4]	0.1691[−4]	0.1691[−4]	0.1691[−4]			0.1664[−4]
0.50	−0.1316[−5]	−0.1295[−5]	0.2964[−3]	0.4523[−3]	0.4607[−3]	0.4607[−3]			0.4651[−3]
0.75	−0.9537[−4]	−0.9361[−4]	0.1444[−2]	0.2303[−2]	0.2545[−2]	0.2548[−2]	0.254[−2]	0.253[−2]	0.2567[−2]
1.00	−0.8408[−3]	−0.8219[−3]	0.2924[−2]	0.5339[−2]	0.6668[−2]	0.6688[−2]	0.664[−2]	0.665[−2]	0.6649[−2]
1.25	−0.3135[−2]	−0.3048[−2]	0.3082[−2]	0.7772[−2]	0.1132[−1]	0.1138[−1]	0.111[−1]	0.113[−1]	0.1103[−1]
1.50	−0.7507[−2]	−0.7255[−2]	0.8326[−3]	0.8099[−2]	0.1463[−1]	0.1474[−1]	0.142[−1]	0.146[−1]	0.1344[−1]

[a]L_{max} was set to 9 for $J=1$.

with different choices of the PS to CF transition radius were made, and it was found that symmetry of the Kohn matrix could be destroyed by an inappropriate choice. Even with the best possible choice of the PS to CF transition, calculations at small k were quite exacting and numerical inaccuracies in the phase shift of up to 1% could easily be present for the smallest values of k given in the tables for each ion. However, the annihilation parameter $Z_{eff}^{(J)}$ was not very sensitive to the exact choice of the PS to CF transition radius.

IV. THE SCATTERING OF POSITRONS FROM He$^+$

A sequence of calculations of different sophistication were performed to give insight into the collision dynamics. These calculation were as follows.

(i) The CWBA as described in the preceding section.

(ii) The one-state close-coupling approximation CC(1) with the electron target states restricted to be the He$^+$ 1s.

(iii) The three-state close-coupling approximation CC(3) with the electron target states restricted to be the He$^+$ 1s, 2s, and 2p states.

(iv) The three-state close-coupling approximation CC($\bar{3}$) with the electron target states restricted to be the He$^+$ 1s, 2s, and $\overline{2p}$ states. The $\overline{2p}$ pseudostate is constructed to recover all of the ground-state dipole polarizability $0.28125a_0^3$.

(v) The CI-Kohn calculation with $L_{max}=8$. This is the largest explicit calculation that was performed and included short-range functions up to $L_{max}=8$. The details of the calculations were slightly different for s-wave and p-wave calculations. A very large number of short-range functions, e.g., about 45, are needed for the positron channels that are dipole coupled to the entrance channel. For the $J=0$ partial wave, this is the $\ell=1$ positron channel. For the $J=1$ partial wave, one needs the large basis for the $\ell=0$ and $\ell=2$ positron orbitals. The $J=1$ calculation extended the partial-wave expansion to $L_{max}=9$ in order to compensate for a more slowly

converging $Z_{eff}^{(1)}$. The exponents of the LTO basis were optimized manually for all the systems by maximizing the phase shift at a momentum of $k=(Z-1)$. These calculations are referred to as the CIKOHN$_8$ (or CIKOHN$_9$) calculations.

(vi) The calculation with $L_{max}\rightarrow\infty$. The limit is determined by using Eqs. (21)–(23) in conjunction with the three calculations with the largest values of L_{max}. These calculations are referred to as the CIKOHN$_\infty$ calculations.

The validity of the programs were tested by a number of checks. First of all, the results of the CC(1) calculation were compared with phase shifts and annihilation parameters computed by a direct integration of the Schrödinger equation by the Numerov method. Next, calculations of electron-He$^+$ scattering in the static-exchange approximation were compared with independent calculations in the same model [28]. Calculations were also performed at two values of τ, $\tau=0$, and $\tau=\pi/2$. The computed phase shifts and Z_{eff} agreed to about five significant digits for all combinations of Z and k reported in the tables with the exception of the lowest k for each ion. Even here, values of Z_{eff} were in agreement to five digits and the differences between the two phase shifts never exceeded 1%. Finally, the algebra related to the inclusion of the Coulomb functions was tested by using this part of the program (with $\eta=0$) to reproduce previous calculations of positron-hydrogen scattering [9].

The phase shifts and Z_{eff} for the $J=0$ and 1 partial waves are listed in Tables III and IV. The present phase shifts are compared with those of Bransden, Noble, and Whitehead (BNW) [4] and the Harris-Nesbet variational results of Gien [5,6]. The results of the Gien E6PS basis are presented. In some instances the BNW and Gien phase shifts are interpolated from their published values. As expected, the phase shifts become more positive as the flexibility of the channel space is increased. The CC(1) phase shifts are most negative, while the $L_{max}=8$ phase shifts are the largest. The extrapolation corrections to the phase shifts are generally small,

TABLE IV. The annihilation parameter, $Z_{eff}^{(J)}$ for positron scattering from He^+. The column k reports momentum in a_0^{-1}. The numbers in square brackets denote powers of 10.

k	CWBA	CC(1)	CC(3)	CC($\bar{3}$)	CIKOHN$_8$[a]	CIKOHN$_\infty$	Model
				$J=0$			
0.25	0.1484[−8]	0.1332[−8]	0.1635[−8]	0.1850[−8]	0.3171[−8]	0.3856[−8]	0.3548[−8]
0.50	0.1977[−3]	0.1756[−3]	0.2119[−3]	0.2394[−3]	0.4176[−3]	0.5026[−3]	0.4715[−3]
0.75	0.7753[−2]	0.6735[−2]	0.8027[−2]	0.9200[−2]	0.1607[−1]	0.1904[−1]	0.1834[−1]
1.00	0.4085[−1]	0.3429[−1]	0.4015[−1]	0.4654[−1]	0.8134[−1]	0.9472[−1]	0.9405[−1]
1.25	0.9744[−1]	0.7886[−1]	0.9033[−1]	0.1051	0.1829	0.2093	0.2142
1.50	0.1577	0.1241	0.1392	0.1613	0.2782	0.3134	0.3299
				$J=1$			
0.25	0.2916[−9]	0.2845[−9]	0.3911[−9]	0.4259[−9]	0.7632[−9]	0.9531[−9]	0.8840[−9]
0.50	0.4495[−4]	0.4379[−4]	0.5818[−4]	0.6321[−4]	0.1166[−3]	0.1450[−3]	0.1365[−3]
0.75	0.2144[−2]	0.2079[−2]	0.2701[−2]	0.3009[−2]	0.5548[−2]	0.6795[−2]	0.6529[−2]
1.00	0.1394[−1]	0.1342[−1]	0.1701[−1]	0.1944[−1]	0.3586[−1]	0.4315[−1]	0.4240[−1]
1.25	0.4077[−1]	0.3883[−1]	0.4809[−1]	0.5621[−1]	0.1038	0.1226	0.1230
1.50	0.7955[−1]	0.7494[−1]	0.9096[−1]	0.1084	0.2003	0.2327	0.2364

[a]L_{max} was set to 9 for $J=1$.

thereby indicating that the convergence of the phase shift with L_{max} is satisfactory.

The agreement of the CIKOHN$_\infty$ phase shifts with the BNW and Gien s-wave phase shifts is generally very good. In some instances the BNW phase shifts are a bit smaller than the Gien phase shifts, in these cases the CIKOHN$_\infty$ phase shifts are in better agreement with the Gien phase shifts. The overall comparison with the Gien results and previous experience on the positron-hydrogen system [9] suggest that CIKOHN$_\infty$ phase shifts are accurate to about 1%. Any residual error will probably lead to the exact phase shifts being underestimated. For most momenta the CIKOHN$_\infty$ phase shifts are more positive than those of Gien and in these cases it is likely that the present phase shifts are slightly more accurate.

The CIKOHN$_\infty$ p-wave phase shifts are also in reasonable agreement with the variational phase shifts of Gien [5,6]. The size of the $L_{max} \rightarrow \infty$ correction is less than 1% at all momenta listed in Table III. The tendency for the CIKOHN$_\infty$ phase shifts to be slightly larger than those of Gien can be taken as an indication that the present phase shifts are slightly more precise.

The uncertainties in the phase shifts are largest at small momenta for two distinct reasons. First, the relative contributions of the polarization interactions to the phase shifts are largest at these momenta. Although the number of short-range basis functions used to describe the positron channel associated with dipole excitations was large, the long range of the dipole interaction does slow convergence. It is possible that incompleteness of the radial basis could lead to errors of order 1%. The other area of uncertainty lies in the accuracy of the regular and irregular Coulomb functions. The numerical procedures used to compute to these functions are most slowly convergent and most susceptible to round-off errors at small values of k.

Some interesting trends are seen when one examines the CC(1)→CC(3)→CC($\bar{3}$)→CIKOHN$_8$→CIKOHN$_\infty$ phase

shifts. First, the phase shift increases monotonically as the sophistication of the calculation increases. Second, the CC($\bar{3}$) phase shift is very close to CIKOHN$_\infty$ phase shift at the lowest momentum. As the momentum increases the differences between these two calculations increases. At the lowest momentum, the positron is less likely to penetrate close to the nucleus, and therefore the dominant atomic effect is the $\alpha_d/(2r^4)$ dipole polarization potential. Since the CC($\bar{3}$) model gives the dipole polarizability exactly, it is expected to give an accurate phase shift very close to threshold. As the energy increases, the positron has a larger probability of penetrating closer to the nucleus and therefore short-range electron-positron correlations become more important.

The annihilation parameter generally shows a tendency to increase in magnitude as the sophistication of the calculation is improved. One salient feature is the stronger contribution made by the extrapolation correction to final values of $Z_{eff}^{(J)}$. The size of the correction was about 15% for $Z_{eff}^{(0)}$. The p-wave annihilation parameter $Z_{eff}^{(1)}$ is more slowly convergent and therefore the calculations were done with L_{max} increased to 9. Even so, the correction constitutes 18% of the final value of $Z_{eff}^{(1)}$ at $k=1.0a_0^{-1}$. If it is assumed that the extrapolation correction itself has an uncertainty of 20%, then the net uncertainty in $Z_{eff}^{(1)}$ could be about 4%.

The most notable feature of the energy dependence of $Z_{eff}^{(0)}$ is its extremely small size of 4×10^{-9} at $k=0.25a_0^{-1}$. This translates to an annihilation cross section of $6 \times 10^{-15}\pi a_0^2$. The small cross section is basically due to $W(\eta)$ which impedes the ability of the positron to tunnel through the repulsive Coulomb potential. As the energy decreases further the annihilation rate becomes minute, and at close to thermal energies, i.e., $k=0.05a_0^{-1}$, considerations based on the CWBA suggest that $Z_{eff}^{(0)}$ should be of order 10^{-51}.

The slower convergence of $Z_{eff}^{(1)}$ was also present for positron-hydrogen scattering [9]. The slow convergence of $Z_{eff}^{(J)}$ is known to result from the strong localization of the

TABLE V. The phase shifts δ_J in radians for positron scattering from Li^{2+}. The column k reports momentum in a_0^{-1}. The numbers in square brackets denote powers of 10.

k	CWBA	CC(1)	CC(3)	CC($\bar{3}$)	CIKOHN$_8$[a]	CIKOHN$_\infty$	Gien (E6PS)	Model
				$J=0$				
0.50	−0.1099[−9]	−0.1085[−9]	0.9746[−5]	0.1482[−4]	0.1483[−4]	0.1483[−4]		0.1513[−4]
1.00	−0.2789[−4]	−0.2678[−4]	0.3206[−3]	0.5093[−3]	0.5389[−3]	0.5391[−3]		0.5502[−3]
1.50	−0.1536[−2]	−0.1458[−2]	0.5074[−3]	0.1841[−2]	0.2565[−2]	0.2575[−2]	0.256[−2]	0.2692[−2]
2.00	−0.1006[−1]	−0.9392[−2]	−0.5311[−2]	−0.1747[−2]	0.1174[−2]	0.1213[−2]	0.116[−2]	0.1225[−2]
2.40	−0.2389[−1]	−0.2203[−1]	−0.1691[−1]	−0.1171[−1]	−0.6595[−2]	−0.6533[−2]	−0.662[−2]	−0.7593[−2]
2.50	−0.2814[−1]	−0.2588[−1]	−0.2061[−1]	−0.1510[−1]	−0.9462[−2]	−0.9396[−2]		−0.1078[−1]
3.00	−0.5189[−1]	−0.4729[−1]	−0.4191[−1]	−0.3539[−1]	−0.2757[−1]	−0.2749[−1]		−0.3189[−1]
				$J=1$				
0.50	−0.101[−10]	−0.120[−10]	0.8867[−5]	0.1349[−4]	0.1349[−4]	0.1349[−4]		0.1357[−4]
1.00	−0.2920[−5]	−0.2894[−5]	0.2271[−3]	0.3486[−3]	0.3595[−3]	0.3596[−3]		0.3647[−3]
1.50	−0.1905[−3]	−0.1883[−3]	0.9096[−3]	0.1561[−2]	0.1796[−2]	0.1799[−2]	0.179[−2]	0.1837[−2]
2.00	−0.1491[−2]	−0.1467[−2]	0.9243[−3]	0.2660[−2]	0.3713[−2]	0.3731[−2]	0.370[−2]	0.3770[−2]
2.40	−0.4052[−2]	−0.3971[−2]	−0.6278[−3]	0.2216[−2]	0.4309[−2]	0.4344[−2]	0.429[−2]	0.4118[−2]
2.50	−0.4928[−2]	−0.4825[−2]	−0.1270[−2]	0.1863[−2]	0.4245[−2]	0.4285[−2]		0.3913[−2]
3.00	−0.1054[−1]	−0.1027[−1]	−0.5930[−2]	−0.8801[−3]	0.2538[−2]	0.2598[−2]		0.7832[−3]

[a]L_{max} was set to 9 for $J=1$.

electron and positron clouds in the vicinity of each other. The presence of the additional centrifugal barrier for the $J=1$ partial-wave results in the region of the maximum electron-positron overlap being further from the nucleus, and thus the maximum angular momentum of the nuclear centered partial-wave expansion of the scattering wave function needs to be increased.

Comment on the extrapolation correction

The major source of uncertainty in the annihilation parameter is the contribution from the extrapolation correction. In order to do this reliably it is necessary to compute Δ and p_Z precisely. This in turn requires calculations for a series of L_{max} that are close to exact. Fortunately, the two major contributions leading to errors from a given calculation tend to cancel each other.

The first source of error is that the value of p_Z does tend to change with L_{max}. The asymptotic value $p_Z=2$ is usually approached from below as L_{max} increases [23]. Typically, p_Z is about 1.80 for most of the calculations reported here. Therefore, this leads to the correction being overestimated.

Another source of error is of course the radial basis. In order to compute the successive increments with L_{max} exactly one needs a radial basis that is complete. Since the increments represent the *difference* between two calculations, any incompleteness in the basis is amplified. We have noticed that p_Z tends to decrease as the dimension of the radial basis is increased. The radial basis used in the present calculations are large, but not complete. This means p_Z tends to be overestimated for any specific calculation with a finite basis. This has been noticed in earlier CI-Kohn calculations of the e^+Cu system [23]. Therefore truncation of the radial basis results in the extrapolation correction being underestimated.

It is noticeable that the relative size of the $L_{max}\rightarrow\infty$ correction for $Z_{eff}^{(J)}$ is largest at the smallest momentum. Previous calculations on neutral targets also had relatively larger $L_{max}\rightarrow\infty$ corrections closer to threshold [9]. This is true for the multiply charged ions as well (refer to Tables VI, VIII, and X). Part of the reason may be due to the fact that the radial basis was optimized at $k=(Z-1)$. A poorer optimization of the LTO exponents for the higher ℓ values at low momenta leads to the successive increments to $Z_{eff}^{(J)}$ decaying too quickly. If this is the case, then $Z_{eff}^{(J)}$ could be systematically too large by a couple of percent at the smallest momenta.

On the other hand, the relative contribution of the $L_{max}\rightarrow\infty$ correction to the phase shift is smallest at small momenta. The repulsive potential prevents the positron from tunneling into the electron charge cloud, and therefore short-range electron-positron correlations are relatively less important in the scattering process (the small size of $Z_{eff}^{(J)}$ is consistent with this explanation).

V. POSITRON SCATTERING FROM MULTIPLY CHARGED IONS

Tables V–X give the phase shifts and annihilation parameters for multiply charged hydrogenic ions Li^{2+}, Be^{4+}, and F^{8+}. The calculations performed used basis sets which were very similar in size to those performed for the He$^+$ system. The exponents of the LTO basis for each ion were reoptimized at $k=(Z-1)$.

The comparison with the phase shifts of Gien [6] for Li^{2+} and B^{4+} is generally very good with agreement at the $1-2\%$ level being typical. Once again, the CIKOHN$_\infty$ phase shifts are slightly more positive than those of Gien, which suggests that they may be slightly more accurate.

TABLE VI. The annihilation parameter, $Z_{eff}^{(J)}$ for positron scattering from Li^{2+}. The column k reports momentum in a_0^{-1}. The numbers in square brackets denote powers of 10.

k	CWBA	CC(1)	CC(3)	CC($\bar{3}$)	CIKOHN$_8$[a]	CIKOHN$_\infty$	Model
				$J=0$			
0.50	0.2560[−8]	0.2433[−8]	0.2829[−8]	0.3018[−8]	0.4298[−8]	0.4890[−8]	0.4539[−8]
1.00	0.3182[−3]	0.2995[−3]	0.3420[−3]	0.3684[−3]	0.5235[−3]	0.5894[−3]	0.5612[−3]
1.50	0.1130[−1]	0.1042[−1]	0.1169[−1]	0.1277[−1]	0.1810[−1]	0.2008[−1]	0.1965[−1]
2.00	0.5323[−1]	0.4767[−1]	0.5243[−1]	0.5774[−1]	0.8159[−1]	0.8913[−1]	0.8982[−1]
2.40	0.1015	0.8882[−1]	0.9632[−1]	0.1062	0.1494	0.1614	0.1662
2.50	0.1136	0.9898[−1]	0.1070	0.1179	0.1657	0.1786	0.1847
3.00	0.1659	0.1423	0.1523	0.1671	0.2337	0.2492	0.2626
				$J=1$			
0.50	0.7991[−9]	0.7888[−9]	0.9987[−9]	0.1039[−8]	0.1468[−8]	0.1706[−8]	0.1638[−8]
1.00	0.1138[−3]	0.1121[−3]	0.1366[−3]	0.1434[−3]	0.2080[−3]	0.2432[−3]	0.2334[−3]
1.50	0.4844[−2]	0.4750[−2]	0.5635[−2]	0.6075[−2]	0.8802[−2]	0.1012[−1]	0.9923[−2]
2.00	0.2765[−1]	0.2691[−1]	0.3118[−1]	0.3440[−1]	0.4979[−1]	0.5625[−1]	0.5632[−1]
2.40	0.6110[−1]	0.5899[−1]	0.6739[−1]	0.7549[−1]	0.1093	0.1218	0.1233
2.50	0.7087[−1]	0.6830[−1]	0.7780[−1]	0.8747[−1]	0.1266	0.1407	0.1472
3.00	0.1222	0.1167	0.1318	0.1526	0.2195	0.2407	0.2426

[a]L_{max} was set to 9 for $J=1$.

The following ordering CC(1)<CWBA<CC($\bar{3}$) <CIKOHN$_\infty$<CIKOHN$_\infty$ of the magnitude of $Z_{eff}^{(J)}$ is rigorously obeyed by all the results given in Tables IV–X. This ordering is a measure of the variational flexibility of the positron basis in allowing the positron to approach the nucleus and overlap with the electron. It is also noticed that the relative difference between the CWBA Z_{eff} and the CIKOHN$_\infty$ estimates of Z_{eff} decreased as Z increased. This is readily seen in Figs. 5 and 6 which are discussed in more detail later.

There was another consistent variation of $Z_{eff}^{(J)}$ with Z. The relative size of the extrapolation correction became less important as Z increased. As the nuclear charge increases, the electron distribution will be closer to the nucleus. Therefore the region where electron-positron correlations are important is located closer to the origin and consequently the convergence of the partial-wave expansion is faster.

Heuristic description of phase-shift behavior

The s-wave phase shifts initially increase as the energy increases from threshold. This is simply explained by consideration of the effective potential for positron-ion scattering.

The residual interaction [after subtraction of the asymptotic $(Z-1)/r$ potential] consists of two parts. At long

TABLE VII. The phase shifts δ_J in radians for positron scattering from B^{4+}. The column k reports momentum in a_0^{-1}. The numbers in square brackets denote powers of 10.

k	CWBA	CC(1)	CC(3)	CC($\bar{3}$)	CIKOHN$_8$	CIKOHN$_\infty$	Gien (E6PS)	Model
				$J=0$				
1.00	−0.1184[−9]	−0.1208[−9]	0.5029[−5]	0.7651[−5]	0.7653[−5]	0.7653[−5]		0.7872[−5]
2.00	−0.2809[−4]	−0.2754[−4]	0.1457[−3]	0.2414[−3]	0.2589[−3]	0.2591[−3]	0.253[−3]	0.2662[−3]
3.00	−0.1416[−2]	−0.1377[−2]	−0.5023[−3]	0.1244[−3]	0.4722[−3]	0.4761[−3]	0.466[−3]	0.4983[−3]
4.00	−0.8485[−2]	−0.8153[−2]	−0.6527[−2]	−0.5022[−2]	−0.3801[−2]	−0.3788[−2]	−0.386[−2]	−0.4174[−2]
5.00	−0.2193[−1]	−0.2088[−1]	−0.1887[−1]	−0.1677[−1]	−0.1459[−1]	−0.1458[−1]		−0.1634[−1]
6.00	−0.3787[−1]	−0.3590[−1]	−0.3412[−1]	−0.3271[−1]	−0.2907[−1]	−0.2905[−1]		−0.3218[−1]
				$J=1$				
1.00	−0.146[−10]	−0.157[−10]	0.6228[−5]	0.6931[−5]	0.6936[−5]	0.6936[−5]		0.7060[−5]
2.00	−0.3901[−5]	−0.3882[−5]	0.1565[−3]	0.1750[−3]	0.1823[−3]	0.1823[−3]	0.176[−3]	0.1861[−3]
3.00	−0.2295[−3]	−0.2280[−3]	0.5505[−3]	0.6176[−3]	0.7476[−2]	0.7492[−3]	0.741[−3]	0.7712[−3]
4.00	−0.1613[−2]	−0.1597[−2]	0.1931[−3]	0.2747[−3]	0.7766[−3]	0.7835[−3]	0.755[−3]	0.7213[−3]
5.00	−0.4834[−2]	−0.4768[−2]	−0.1876[−2]	−0.1782[−2]	−0.7065[−3]	−0.6930[−3]		−0.1451[−2]
6.00	−0.9506[−2]	−0.9348[−2]	−0.5576[−2]	−0.4556[−2]	−0.5067[−2]	−0.5052[−2]		−0.5838[−2]

TABLE VIII. The annihilation parameter $Z_{eff}^{(J)}$ for positron scattering from B^{4+}. The column k reports momentum in a_0^{-1}. The numbers in square brackets denote powers of 10.

k	CWBA	CC(1)	CC(3)	CC($\bar{3}$)	CIKOHN$_8$	CIKOHN$_\infty$	Model
				$J=0$			
1.00	0.3965[−8]	0.3873[−8]	0.4275[−8]	0.4413[−8]	0.5416[−8]	0.5838[−8]	0.5490[−8]
2.00	0.4567[−3]	0.4432[−3]	0.4812[−3]	0.5021[−3]	0.6150[−3]	0.6583[−3]	0.6293[−3]
3.00	0.1468[−1]	0.1404[−1]	0.1500[−1]	0.1582[−1]	0.1931[−1]	0.2045[−1]	0.1997[−1]
4.00	0.6242[−1]	0.5849[−1]	0.6165[−1]	0.6531[−1]	0.7946[−1]	0.8330[−1]	0.8305[−1]
5.00	0.1214	0.1119	0.1168	0.1237	0.1500	0.1559	0.1582
6.00	0.1640	0.1502	0.1545	0.1577	0.1969	0.2033	0.2118
				$J=1$			
1.00	0.1626[−8]	0.1616[−8]	0.1821[−8]	0.1876[−8]	0.2329[−8]	0.2561[−8]	0.2433[−8]
2.00	0.2129[−3]	0.2113[−3]	0.2391[−3]	0.2451[−3]	0.3037[−3]	0.3314[−3]	0.3184[−3]
3.00	0.8109[−2]	0.8016[−2]	0.9139[−2]	0.9291[−2]	0.1149[−1]	0.1239[−1]	0.1210[−1]
4.00	0.4122[−1]	0.4049[−1]	0.4657[−1]	0.4695[−1]	0.5795[−1]	0.6174[−1]	0.6110[−1]
5.00	0.9486[−1]	0.9257[−1]	0.1079	0.1084	0.1346	0.1420	0.1395
6.00	0.1489	0.1446	0.1697	0.1792	0.1989	0.2081	0.2174

distances there is the adiabatic polarization potential which is written as $V \sim -\alpha_d/(2r^4)$. The polarization potential is largest at the edge of the ground-state charge distribution. Then there is the increased nuclear repulsion that is seen whenever the positron is inside the electron charge distribution.

The attractive interaction is the more important term at low energies. The asymptotic $(Z-1)/r$ repulsion acts to keep the incident positron away from the interior region of the target. Therefore, the increased nuclear repulsion has a small impact on the phase shift since the amplitude of the scattering wave function is small here. However, as the kinetic energy of the positron increases, it is more likely to tunnel through the Coulomb barrier into the inner region of the atom. When this occurs, the increased nuclear repulsion starts to have an impact and the phase shift then becomes negative.

The maximum positive value of the phase shift is quite small for all the systems considered. This is not surprising since the polarizability $\alpha_d = 4.5/Z^4$ is small for $Z \geqslant 2$. Since the polarizability decreases as Z increases it would be expected that the magnitude of the phase shift at its maximum positive value should decrease as Z increases, and this is what happens.

Research on atomic systems [9,20,29–31] has shown that there is a dynamical connection between the size of the low-energy phase shifts and the annihilation parameter. An attractive interaction leads to the amplitude of the wave function being larger close to the origin, and therefore can be expected to increase the annihilation parameter. However, the maximum positive value of the phase shift obtained in all the calculations was no larger than 0.015 rad. The small size of the phase shift suggests that the effective polarization poten-

TABLE IX. The phase shifts δ_J in radians for positron scattering from F^{8+}. The column k reports momentum in a_0^{-1}. The numbers in square brackets denote powers of 10.

k	CWBA	CC(1)	CC(3)	CC($\bar{3}$)	CIKOHN$_8$	CIKOHN$_\infty$	Model
				$J=0$			
2.00	−0.958[−10]	−0.940[−10]	0.1941[−5]	0.2952[−5]	0.2954[−5]	0.2954[−5]	0.3011[−5]
4.00	−0.2152[−4]	−0.2131[−4]	0.4289[−4]	0.7884[−4]	0.8600[−4]	0.8605[−4]	0.8956[−4]
6.00	−0.1015[−2]	−0.9996[−3]	−0.6980[−3]	−0.4745[−3]	−0.3501[−3]	−0.3489[−3]	−0.3470[−3]
8.00	−0.5709[−2]	−0.5585[−2]	−0.5056[−2]	−0.4555[−2]	−0.4152[−2]	−0.4148[−2]	−0.4366[−2]
10.00	−0.1401[−1]	−0.1363[−1]	−0.1310[−1]	−0.1238[−1]	−0.1175[−1]	−0.1175[−1]	−0.1242[−1]
12.00	−0.2323[−1]	−0.2257[−1]	−0.2183[−1]	−0.2114[−1]	−0.2182[−1]	−0.2181[−1]	−0.2162[−1]
				$J=1$			
2.00	−0.139[−10]	−0.135[−10]	0.1756[−5]	0.2647[−5]	0.2650[−5]	0.2650[−5]	0.2702[−5]
4.00	−0.3486[−5]	−0.3477[−5]	0.4020[−4]	0.6376[−4]	0.6692[−4]	0.6693[−4]	0.6904[−4]
6.00	−0.1900[−3]	−0.1893[−3]	−0.3236[−5]	0.1175[−3]	0.1675[−3]	0.1680[−3]	0.1787[−3]
8.00	−0.1240[−2]	−0.1233[−2]	−0.8712[−3]	−0.5771[−3]	−0.4015[−3]	−0.3994[−3]	−0.4429[−3]
10.00	−0.3487[−2]	−0.3459[−2]	−0.2871[−2]	−0.2387[−2]	−0.2190[−2]	−0.2187[−2]	−0.2435[−2]
12.00	−0.6510[−2]	−0.6448[−2]	−0.5263[−2]	−0.4537[−2]	−0.4804[−2]	−0.4800[−2]	−0.5436[−2]

TABLE X. The annihilation parameter, $Z_{\text{eff}}^{(J)}$ for positron scattering from F^{8+}. The column k reports momentum in a_0^{-1}. The numbers in square brackets denote powers of 10.

k	CWBA	CC(1)	CC(3)	CC($\bar{3}$)	CIKOHN$_8$	CIKOHN$_\infty$	Model
				$J=0$			
2.00	0.5302[−8]	0.5244[−8]	0.5556[−8]	0.5639[−8]	0.6306[−8]	0.6585[−8]	0.6303[−8]
4.00	0.5749[−3]	0.5664[−3]	0.5933[−3]	0.6072[−3]	0.6777[−3]	0.7030[−3]	0.6813[−3]
6.00	0.1715[−1]	0.1674[−1]	0.1735[−1]	0.1787[−1]	0.1990[−1]	0.2050[−1]	0.2015[−1]
8.00	0.6787[−1]	0.6546[−1]	0.6732[−1]	0.6951[−1]	0.7721[−1]	0.7911[−1]	0.7873[−1]
10.00	0.1243	0.1188	0.1214	0.1258	0.1389	0.1417	0.1427
12.00	0.1599	0.1526	0.1548	0.1603	0.1727	0.1755	0.1831
				$J=1$			
2.00	0.2525[−8]	0.2517[−8]	0.2736[−8]	0.2738[−8]	0.3079[−8]	0.3253[−8]	0.3175[−8]
4.00	0.3097[−3]	0.3084[−3]	0.3300[−3]	0.3351[−3]	0.3762[−3]	0.3940[−3]	0.3892[−3]
6.00	0.1086[−1]	0.1079[−1]	0.1139[−1]	0.1172[−1]	0.1313[−1]	0.1365[−1]	0.1362[−1]
8.00	0.5095[−1]	0.5042[−1]	0.5276[−1]	0.5479[−1]	0.6133[−1]	0.6334[−1]	0.6363[−1]
10.00	0.1094	0.1078	0.1134	0.1187	0.1308	0.1341	0.1360
12.00	0.1622	0.1594	0.1704	0.1858	0.1950	0.1994	0.2009

tial has a relatively minor influence upon the size of the annihilation parameter. This point will be verified later.

VI. MODEL POTENTIAL DESCRIPTION

In this section a model potential description of the positron-ion collision is presented using the method of Mitroy and co-workers [29,32]. The effective Hamiltonian for the positron moving in the field of the ion is approximated by the model potential,

$$H = -\tfrac{1}{2}\nabla_0^2 + V_{dir}(\mathbf{r}_0) + V_{pol}(\mathbf{r}_0). \qquad (47)$$

The repulsive direct potential V_{dir} is computed from the ground-state wave function of the target ion. The polarization potential is given the form

$$V_{pol}(\mathbf{r}_0) = -\frac{\alpha_d[1 - \exp{(-r^6/\rho^6)}]}{2r^4}, \qquad (48)$$

where $\alpha_d = 4.5/Z^4 a_0^3$ for the hydrogenic ions.

The adjustable parameter ρ is fixed by tuning the model potential phase shift to give a reasonable fit to the CIKOHN$_\infty$ phase shifts. Values of ρ are given in Table XI. The phase shifts from the model potential calculation are tabulated in Tables III, V, VII, and IX. The model potential phase shifts track the CIKOHN$_\infty$ phase shifts reasonably well although there is a tendency for the model potential phase shifts to be slightly too negative at the largest momenta.

TABLE XI. The parameters of the model potential.

Ion	$\rho(a_0)$	G_0	G_1
He$^+$	1.218	2.52	3.00
Li^{2+}	0.837	1.83	2.05
B^{4+}	0.540	1.41	1.50
F^{8+}	0.310	1.20	1.26

The annihilation of positrons in the model is written as [29]

$$Z_{\text{eff}}^{(J)} = \int d^3r\, G_J \rho_{1s}(\mathbf{r}) |\Phi_J(\mathbf{r})|^2, \qquad (49)$$

where $\rho_{1s}(\mathbf{r})$ is the electron density of the $1s$ ground state and $\Phi_J(\mathbf{r})$ is the positron scattering function for the scattering wave function with angular momentum J. The enhancement factor G_J is introduced to take into consideration the impact that electron-positron correlations have in increasing the annihilation rate. In previous works, a common value of J was adopted for all partial waves. A different enhancement factor was adopted for the different partial waves because calculations revealed that G_1 was consistently bigger than G_0. This is understandable since the centrifugal barrier will lead to p-wave annihilation occurring at larger values of r than s-wave annihilation. Therefore, the nuclear Coulomb potential Z/r will have less impact in disrupting electron-positron localization. Enhancement factors are often used in the calculation of the annihilation rate of positrons in condensed-matter systems [33–35].

The valence enhancement factor G_J is computed by the simple identity

$$G_J = \frac{Z_{\text{eff}}^{(J)\text{Kohn}}}{Z_{\text{eff}}^{(J)\text{model}}}, \qquad (50)$$

where $Z_{\text{eff}}^{(J)\text{Kohn}}$ is the annihilation rate of the positron with the valence orbitals as given by the CIKOHN$_\infty$ calculation and $Z_{\text{eff}}^{(J)\text{model}}$ is the annihilation rate predicted by the model potential calculation with $G_J=1$. Values of G_J are listed in Table XI. The model potential phase shifts and $Z_{\text{eff}}^{(J)}$ are listed in Tables III–X. The deviation from the CIKOHN$_\infty$ values of $Z_{\text{eff}}^{(J)}$ does not exceed 10% for any of the entries in Tables IV, VI, VIII, and X. This is an impressive result

TABLE XII. The total Z_{eff} for a number of ions at different values of $1/\eta = k/(Z-1)$. The CIKOHN$_\infty$ values are used for $Z_{eff}^{(0)}$ and $Z_{eff}^{(1)}$; and the higher partial-wave contributions from $J=2$, 3, and 4 are taken from the model potential using the parameters ρ and G_1 of Table XI. The numbers in square brackets denote powers of 10.

$1/\eta$	He$^+$	Li^{2+}	B^{4+}	F^{8+}
0.25	0.484[−8]	0.670[−8]	0.861[−8]	0.102[−7]
0.50	0.655[−3]	0.835[−3]	0.103[−2]	0.116[−2]
0.75	0.264[−1]	0.318[−1]	0.355[−1]	0.378[−1]
1.00	0.144	0.159	0.166	0.168
1.25	0.357	0.369	0.365	0.353
1.50	0.613	0.606	0.552	0.528

when one considers that the calculations for F^{8+} go up to about 1000 eV positron energy.

Table XII gives the total Z_{eff} at the common values of $1/\eta$ for the four different ions. The CIKOHN$_\infty$ calculations of $Z_{eff}^{(J)}$ are used for the $J=0$ and $J=1$ partial waves. The contributions from $J=2,3$, and 4 used Eq. (49) with $G_J=G_1$. An estimate of the importance of the higher J values can be gauged by comparison of Table XII with $Z_{eff}^{(J)}$ given in Tables IV, VI, VIII, and X. The difference between the sum of $Z_{eff}^{(0)}$ and $Z_{eff}^{(1)}$ and Z_{eff} in Table XII is due to the contribution from the higher partial waves. The relative contribution from the higher partial waves is largest at the highest momentum, but even here it does not exceed 25%. The partial-wave sum for Z_{eff} converges quickly with J and the $J=4$ term makes a contribution of 1% or less.

VII. ON THE NATURE OF ANNIHILATION ENHANCEMENT

The electron-positron interaction modifies the scattering wave function in two respects.

(i) The attractive polarization potential leads to positive phase shifts at threshold. This implies an increase in the positron charge density in the vicinity of the target electron charge distribution. This will be referred to as the *overlap* enhancement and there are a number of studies of positron-atom scattering showing the correlation between a large scattering length and a large threshold Z_{eff}. As an aside, it is worth remarking that it is the vanishingly small overlap between the electron and positron wave functions for positive ions at thermal energies that leads to the minute Z_{eff} at these energies.

(ii) The attractive nature of the electron-positron interaction leads to a localization of the positron in the vicinity of the electron. This effect will be called the *clustering* effect and is well known in condensed-matter systems [33,34], positron-atom scattering systems [20,29,30,36], and positron-atom bound states [19,37].

The Li^{2+} model potential calculation at $k=2.0$ has been repeated with the polarization potential set to zero. When this is done, the phase shifts change from $\delta_0 = 0.116 \times 10^{-2}$ rad to $\delta_0 = -0.939 \times 10^{-2}$ rad and from $\delta_1 = 0.376 \times 10^{-2}$ rad to $\delta_1 = -0.147 \times 10^{-2}$ rad. The phase shifts have changed sign al-
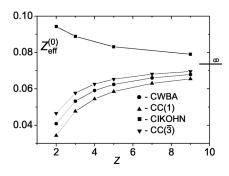

FIG. 5. The s-wave annihilation parameter $Z_{eff}^{(0)}$ at $\eta=1.0$ as a function of Z for various approximations: ●, CWBA; ▲, CC(1); ▼, CC($\bar{3}$); ■, CIKOHN$_\infty$. The horizontal line across the right axis denotes the $Z=\infty$ value for the CWBA.

though the absolute changes are small. However, the annihilation parameters changed from $Z_{eff}^{(0)}=0.0883$ to $Z_{eff}^{(0)}=0.0858$ and from $Z_{eff}^{(1)}=0.0495$ to $Z_{eff}^{(1)}=0.0484$. The net decrease in the annihilation parameter is about 4% for the s wave and 2% for the p wave. Although the polarization potential does increase the positron density in the vicinity of the nucleus (e.g., the positive phase shifts) it has a minimal effect upon the annihilation rate. The minor increase caused by the overlap effect demonstrates that the cluster effect is the dominant cause of the annihilation enhancement for positron scattering from positive ions.

This partly explains the ability of the model with a simple scaling factor to reproduce the more sophisticated variational calculation. In effect, the relative unimportance of overlap enhancement in increasing the annihilation parameter means that it is not sensitive to the fine details of the polarization potential. The rapid variation in the annihilation parameter as the positron energy approaches threshold is largely driven by kinematic factors related to the ability of the positron to tunnel into the repulsive Coulomb barrier.

There are some numerical regularities present in Table XI. The product $(G_J-1)(Z-1)$ is almost constant for all the different ions. The product is approximately equal to 1.5 for $J=0$ and approximately equal to 2.0 for $J=2$. The values of ρ scale roughly as $1/Z$. Since the specific value of ρ does not have much impact on $Z_{eff}^{(J)}$, it should be possible to apply the present model to predict values of $Z_{eff}^{(J)}$ for other ions. The choices $\rho \approx 2.5/Z$, and $G_0 \approx 1+1.50/(Z-1)$ and $G_J=G_1 \approx 1+2.0/(Z-1)$ would seem to be reasonable.

Figure 5 plots $Z_{eff}^{(0)}$ versus Z at constant η. The CWBA result increases monotonically from $Z=2$ to $Z=9$. This can be easily explained by reference to the relative size of the classical turning radius r_c to the mean orbital radius $\langle r \rangle = 1.5/Z$ of the ground-state hydrogenic ion at constant η. At $Z=2$ the ratio $Zr_c/1.5$ is 8/3, which decreases to 4/3 as $Z \rightarrow \infty$. The tendency for the positron to penetrate deeper into the electron cloud as Z increases (η constant) explains the tendency for $Z_{eff}^{(0)}$ to increase. However, the CIKOHN$_\infty$ calculation shows a tendency to decrease as Z increases. The ability of electron-positron correlations to increase the annihilation rate diminishes as Z increases. The stronger Coulomb field of the target inhibits electron-positron localization and therefore Z_{eff} enhancement due to the clustering effect will decrease.
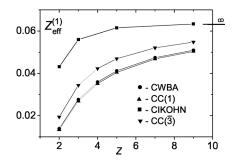
FIG. 6. The p-wave annihilation parameter $Z_{eff}^{(1)}$ at $\eta = 1.0$ as a function of Z for various approximations: $\bullet$, CWBA; $\blacktriangle$, CC(1); $\blacktriangledown$, CC($\bar{3}$); $\blacksquare$, CIKOHN$_\infty$. The horizontal line across the right axis denotes the $Z = \infty$ value for the CWBA.

The plot of $Z_{eff}^{(1)}$ versus Z shown in Fig. 6 shows some differences in qualitative behavior from the s-wave plot. The p-wave CWBA plot is reminiscent of the s-wave plot; $Z_{eff}^{(1)}$ increases monotonically from $Z=2$ to $Z=9$. Once again, the relative size of the classical turning radius to the mean orbital radius, i.e., $Zr_c/1.5$ decreases as Z increases at constant η. But, unlike the case for $J=0$, the CIKOHN$_\infty$ result shows a tendency to increase with increasing Z. This is a consequence of the centrifugal barrier which acts to suppress the ability of the positron to penetrate into the electron cloud. The relative importance of the centrifugal barrier is stronger at smaller values of Z. Therefore, the p-wave CWBA value increases by a factor of 3.6 from $Z=2$ to $Z=9$ while the corresponding increase in the s-wave CWBA value of $Z_{eff}^{(J)}$ was only a factor of 1.5. The tendency for the p-wave CWBA to increase more quickly with increasing Z overwhelms the tendency for the clustering effect to decrease with increasing Z and the net effect is a $Z_{eff}^{(1)}$ that decreases with increasing Z.

VIII. CONCLUSIONS

The Kohn variational method using nuclear centered basis functions has been applied to the calculation of the phase shifts and annihilation parameters for positron scattering from hydrogenlike ions. The phase shifts agree very well with those of a previous variational calculation by Gien [5,6] for those ions and momenta common to both calculations and demonstrate that the CI-Kohn approach is capable of obtaining phase shifts comparable in accuracy to calculations which explicitly include the electron-positron distance in the scattering wave function. Indeed, we believe that the present phase shifts are marginally more accurate than those of Gien since they are slightly more positive. Besides giving close to converged phase shifts, results are also presented for a number of less sophisticated models which restrict the allowable excitations of the target electron. Such calculations are useful as benchmarks in developing alternative methods to compute positron-ion scattering.

In common with other positron scattering calculations with a single-center basis it is found that the convergence is slow with respect to the maximum orbital angular momenta of the basis states included in the partial-wave expansion of the wave function. The convergence problems were not as severe as for neutral systems since the region of strong electron-positron localization occurs closer to the origin. It is found that convergence of the annihilation parameter is slower for p-wave than for s-wave scattering. This is compatible with earlier calculations for neutrals and suggests the electron-positron localization occurs further from the origin due to the presence of the centrifugal barrier.

However, extrapolations in angular momentum were needed in order to mopup the last $0.1-2\%$ of the phase shift and the last $5-20\%$ of the annihilation parameter. While the extrapolation correction is probably the largest source of error in the tabulated phase shifts and annihilation parameters, it should be noted that a 20% error in the $Z_{eff}^{(J)}$ extrapolation correction would only lead to a 4% error in the final value of $Z_{eff}^{(J)}$.

One of the more interesting results of the present work is the importance of cluster enhancement of the positron annihilation rate even for strong Coulomb fields. Even for the heavily ionized F^{8+} system, there is still a 20% enhancement. The annihilation parameter at thermal energies is microscopically small due to the diminishing amplitude of the positron wave function as it tunnels through the repulsive Coulomb barrier. This means that losses due to annihilation do not have to be considered in cooling schemes involving positive ions and positrons [38–41].

ACKNOWLEDGMENTS

[1] J. Mitroy, J. Phys. B **26**, L625 (1993).

[2] J. Mitroy, Aust. J. Phys. **46**, 751 (1993).

[3] I. Shimamura, J. Phys. Soc. Jpn. **31**, 217 (1971).

[4] B. H. Bransden, C. J. Noble, and R. J. Whitehead, J. Phys. B **34**, 2267 (2001).

[5] T. T. Gien, J. Phys. B **34**, L535 (2001).

[6] T. T. Gien, J. Phys. B **34**, 5103 (2001).

[7] E. A. G. Armour and J. W. Humberston, Phys. Rep. **204**, 165 (1991).

[8] A. K. Bhatia, A. Temkin, R. J. Drachman, and H. Eiserike, Phys. Rev. A **3**, 1328 (1971).

[9] M. W. J. Bromley and J. Mitroy, Phys. Rev. A **67**, 062709 (2003).

[10] W. Kohn, Phys. Rev. **71**, 902 (1947).

[11] J. Callaway, Phys. Rep. **45**, 89 (1978).

[12] R. K. Nesbet, *Variational Methods in Electron-Atom Scatter-*

ing Theory (Plenum, New York, 1980).

[13] P. G. Burke and C. J. Joachain, *Theory of Electron-Atom Collisions. Part 1 Potential Scattering* (Plenum, New York, 1995).

[14] T. Kato, Phys. Rev. **80**, 475 (1950).

[15] S. I. Rubinow, Phys. Rev. **98**, 183 (1955).

[16] P. A. Fraser, Adv. At. Mol. Phys. **4**, 63 (1968).

[17] R. P. McEachran, D. L. Morgan, A. G. Ryman, and A. D. Stauffer, J. Phys. B **10**, 663 (1977).

[18] G. G. Ryzhikh and J. Mitroy, J. Phys. B **33**, 2229 (2000).

[19] J. Mitroy, M. W. J. Bromley, and G. G. Ryzhikh, J. Phys. B **35**, R81 (2002).

[20] V. A. Dzuba, V. V. Flambaum, G. F. Gribakin, and W. A. King, J. Phys. B **29**, 3151 (1996).

[21] G. Gribakin and J. Ludlow, J. Phys. B **35**, 339 (2002).

[22] M. W. J. Bromley and J. Mitroy, Phys. Rev. A **65**, 062506 (2002).

[23] M. W. J. Bromley and J. Mitroy, Phys. Rev. A **66**, 062504 (2002).

[24] *Handbook of Mathematical Functions*, Natl. Bur. Stand. Appl. Math. Ser. No. 55, edited by M. Abramowitz and I. E. Stegun (U.S. GPO, Washington, D.C., 1972).

[25] L. D. Landau and E. M. Lifshitz, *Quantum Mechanics (Non-Relativistic Theory)* (Pergamon, Oxford, 1977), Vol. 3.

[26] M. J. Seaton, Comput. Phys. Commun. **146**, 250 (2002).

[27] A. R. Barnett, in *Computational Atomic Physics, Electron and Positron Collisions*, edited by K. Bartschat (Springer, Berlin, 1996), p. 181.

[28] N. Maleki, Phys. Rev. A **29**, 2470 (1983).

[29] J. Mitroy and I. A. Ivanov, Phys. Rev. A **65**, 042705 (2002).

[30] G. F. Gribakin, Phys. Rev. A **61**, 022720 (2000).

[31] J. Mitroy, Phys. Rev. A **66**, 022716 (2002).

[32] M. W. J. Bromley, J. Mitroy, and G. Ryzhik, J. Phys. B **31**, 4449 (1998).

[33] E. Boronski and R. M. Nieminen, Phys. Rev. B **34**, 3820 (1986).

[34] M. J. Puska and R. M. Nieminen, Rev. Mod. Phys. **66**, 841 (1994).

[35] B. Barbiellini, in *New Directions in Antimatter Physics and Chemistry*, edited by C. M. Surko and F. A. Gianturco (Kluwer Academic, Dordrecht, 2001), p. 127.

[36] V. A. Dzuba, V. V. Flambaum, W. A. King, B. N. Miller, and O. P. Sushkov, Phys. Scr. **46**, 248 (1993).

[37] G. G. Ryzhikh, J. Mitroy, and K. Varga, J. Phys. B **31**, 3965 (1998).

[38] L. H. Haarsma, K. Abdullah, and G. Gabrielse, Phys. Rev. Lett. **75**, 806 (1994).

[39] N. Oshima, T. M. Kojima, M. Niigaki, A. Mohri, K. Komaki, Y. Iwai, and Y. Yamazaki, Nucl. Instrum. Methods Phys. Res. B **205**, 178 (2003).

[40] D. J. Wineland, C. S. Wiener, and J. J. Bollinger, Hyperfine Interact. **76**, 115 (1993).

[41] B. M. Jelenkovic, A. S. Newbury, J. J. Bollinger, W. M. Itano, and T. B. Mitchell, Phys. Rev. A **67**, 063406 (2003).